nature nanotechnology

LETTERS

PUBLISHED ONLINE: 18 JANUARY 2009 | DOI: 10.1038/NNANO.2008.393

A smart dust biosensor powered by kinesin motors

Thorsten Fischer, Ashutosh Agarwal and Henry Hess*

Biosensors can be miniaturized by either injecting smaller volumes into micro- and nanofluidic devices or immersing increasingly sophisticated particles known as 'smart dust' into the sample. The term 'smart dust' originally referred to cubic-millimetre wireless semiconducting sensor devices that could invisibly monitor the environment in buildings and public spaces[1], but later it also came to include functional micrometre-sized porous silicon particles used to monitor yet smaller environments[2,3]. The principal challenge in designing smart dust biosensors is integrating transport functions with energy supply into the device. Here, we report a hybrid microdevice that is powered by ATP and relies on antibody-functionalized microtubules and kinesin motors to transport the target analyte into a detection region. The transport step replaces the wash step in traditional double-antibody sandwich assays. Owing to their small size and autonomous function, we envision that large numbers of such smart dust biosensors could be inserted into organisms or distributed into the environment for remote sensing.

The successful integration of ATP-consuming biomolecular motors[4–8] into synthetic environments enables the transfer of mass transport functions from external pumps to components of biological origin[9,10]. A well-studied nanoscale transport system, termed a 'molecular shuttle' (ref. 11), uses kinesin motors adhered to surfaces to move microtubules functionalized with antibodies for specific capture and transport of antigens[12–18]. This system is fuelled by ATP, and the activation and transport velocity of the molecular shuttle are controlled remotely by photolysis of caged ATP[19,20].

Here, a microdevice is demonstrated that replaces the capture–wash–tag–wash–detect sequence in traditional double-antibody-sandwich (DAS) assays with a capture–transport–tag–transport–detect sequence relying on molecular shuttles (Fig. 1). We capture streptavidin and gluthathione-S-transferase (GST) from solution with functionalized microtubules, move the target-coated microtubules until they bind fluorescent markers, and further move the microtubules carrying both target and marker to a separate location. We envision that this capture–transport–tag–transport–detect sequence can serve as the basis of a smart dust microdevice that can be fabricated in large numbers, stored in an inactivated state[21,22], reconstituted, distributed in an aqueous solution, activated by light, and finally read out by stand-off fluorescence detection.

To reduce the detection time, a balance between the time required for the analyte to slowly diffuse to a surface-bound microtubule[23] and the time required for the microtubule to move quickly on a diffusive trajectory[24] to the boundary of the cell is required, suggesting that a flat device is desirable. After additional consideration of assembly and imaging processes, the height and diameter of the device were chosen as 20 and 800 μm, respectively (~10 nl sample volume). The bottom surface comprised a coverslip to enable the observation of the internal processes by fluorescence microscopy. The sidewalls were formed from thick (20 μm), photolithographically patterned SU8 photoresist, which exhibits low autofluorescence[5]. The chosen SU8 processing conditions resulted in an extended 'overhang' at the sidewall and immobilization of gliding microtubules as they contacted the sidewall (see Methods).

Controlled activation of motor-driven transport within the device relies on photolysis of (1-(4,5-dimethoxy-2-nitrophenyl)ethyl)-caged ATP (DMNPE-caged ATP), which is here provided by a UV lamp. However, sunlight can effectively serve the same purpose[19].

Selective recognition of the analyte by both molecular shuttles and optical tags is required to realize the DAS assay. In a first set of experiments, a simplified system was used in which biotinylated microtubules act as molecular shuttles, streptavidin as the analyte, and biotinylated fluorescent nanospheres as the optical tags. In a second set of experiments, a commercially available pair of antibodies for GST was used to create a true DAS. In this system, the biotinylated GST antibody was linked via streptavidin to biotinylated microtubules, GST serving as the analyte and quantum dots conjugated to the second GST antibody serving as the optical tag. In both experiments the distinction between the zones for analyte pick-up and tagging was abolished for three reasons. First, it is permissible for the analyte to bind to the antibody on the tag first and then to the antibody on the gliding shuttle. Second, a sufficient number of encounters between shuttles and tags still occurs. Third, the device assembly process is dramatically simplified.

The experimental results for the streptavidin system are shown in Fig. 2. The photoresist structure was fabricated on a glass coverslip and placed in a humidified chamber. The internal surfaces were coated with casein and kinesin before a solution containing biotinylated, rhodamine-labelled microtubules and a solution of biotinylated 40 nm polystyrene nanospheres was added. The large overhang at the wall prevents the deposition of microtubules and nanospheres within 16 μm of the wall. By means of solution exchanges, streptavidin was added to a final concentration of 1 nM, and subsequently the caged ATP in the solution photolysed by a 90 s pulse of UV light. Microtubules begin to move, collide with nanospheres on the surface, pick up the nanospheres if streptavidin is present on either nanosphere or microtubule, and eventually reach the wall (see Supplementary Information, Figs S1,S2) where their accumulation can be imaged (Fig. 2a,d,g; images false-coloured red). Within hours (see Supplementary Information, Fig. S3), the microtubules, together with their cargo of nanospheres, are deposited at the wall, creating a distinct, new band of fluorescent particles indicative of the presence of streptavidin in the solution (Fig. 2b,e; images false-coloured green). The overlays in Fig. 2c,f,i demonstrate the co-localization between nanospheres and microtubules at the wall.

In a second set of experiments, GST (4 nM) was captured and detected by a commercially available combination of a biotinylated antibody and a quantum dot-conjugated antibody (Fig. 3). Because the antibody-labelled quantum dots did not adhere to the surface, they were dispersed together with the caged ATP in the solution. In solution, quantum dots are invisible to our imaging system because they are out of focus and rapidly diffusing. The observed analyte-dependent deposition of quantum dots (Fig. 3b,e; images false-coloured green) as

University of Florida, Department of Materials Science and Engineering, 160 Rhines Hall, Gainesville, Florida 32611-6400, USA; *e-mail: hhess@mse.ufl.edu

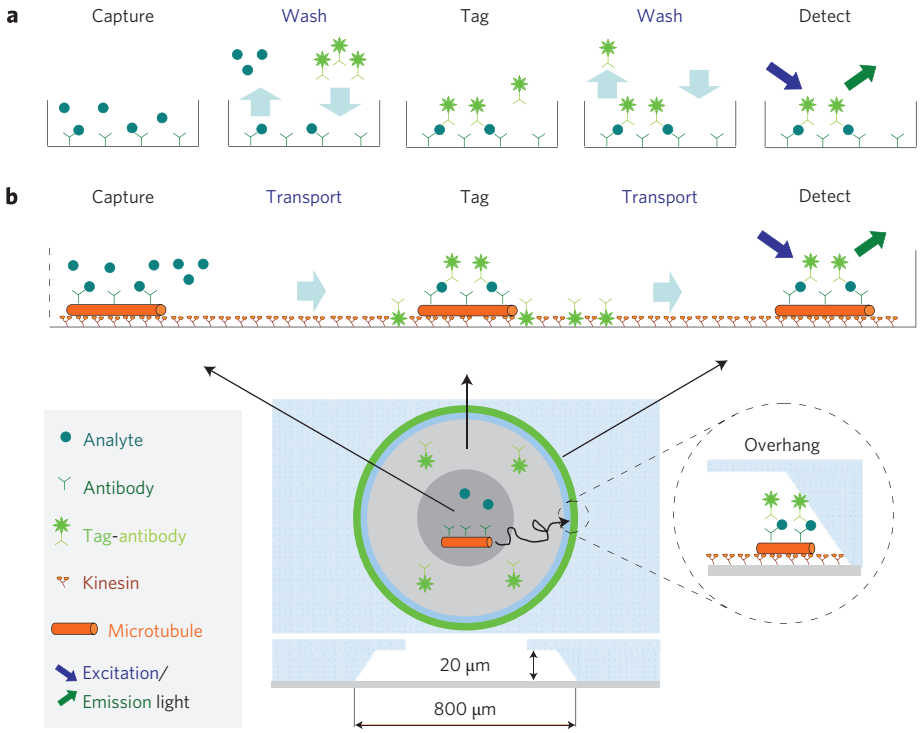

Figure 1 | Concept of a smart dust device using active transport by molecular shuttles. a, The capture–wash–tag–wash–detect sequence of a traditional double-antibody sandwich (DAS) assay. **b**, The capture–transport–tag–transport–detect sequence of the smart dust device, in which antibodies on microtubules capture antigens from solution. Kinesin motors are activated, and collisions of antigen-loaded, gliding microtubules with fluorescent particles functionalized with a second antibody lead to pick-up and transfer of the fluorescent tags to the detection zone, indicating the presence of antigen. A basic device layout comprises a circular well created in photoresist on a coverslip. Analyte harvesting, tagging and detection are performed in different radial zones.

microtubules accumulate at the wall after the activation of the device (Fig. 3a,d; images false-coloured red) confirms the formation and active transport of a DAS of antibody-functionalized microtubules, GST and antibody-functionalized quantum dots. Again, Fig. 3c,f demonstrates the co-localization between quantum dots and microtubules at the wall. The autofluorescence of the photoresist is absolutely and relatively stronger in these images, due to the short excitation wavelength and the low brightness of the quantum dots, respectively.

Control experiments (see Supplementary Information for details) were carried out and verified the specificity of the sensor. For the streptavidin system, nanospheres were deposited in densities of $0.40 \pm 0.04\ \mu m^{-2}$ in the presence and $0.083 \pm 0.008\ \mu m^{-2}$ in the absence of the analyte within the first 16 μm of the wall. For the GST system, the corresponding quantum dot densities were $0.12 \pm 0.01\ \mu m^{-2}$ and $0.0016 \pm 0.0011\ \mu m^{-2}$. The paired Student's *t*-test for the specificity of streptavidin detection and GST detection yielded two-tailed *P*-values of 0.05 and 0.04, respectively.

It was also verified that optical tags were deposited in the detection zone primarily by active transport and not by diffusion. For the streptavidin system, nanospheres adhered strongly to the sensor surface and did not remain in solution; hence, diffusion of nanospheres did not contribute to the observed accumulation during device operation beyond the initial deposition of nanospheres in the detection zone at a density of $0.074 \pm 0.007\ \mu m^{-2}$ during device assembly. For the GST system, the contribution of diffusion to the signal was measured by accumulating microtubules first in the detection zone, and then introducing the analyte. It was found that diffusion contributes a quantum dot density of $0.018 \pm 0.005\ \mu m^{-2}$ during device operation (15% of the total signal).

Although the signal strength of the device needs to be significantly improved to enable remote detection[26], this is the first time that capture of unlabelled analyte by molecular shuttles has been integrated with tagging, transport and localized deposition. As a result, the demonstrated device concept represents a significant advance with respect to previous demonstrations of conceptual building blocks, such as analyte capture by antibody-coated microtubules[12,13], selective pick-up of tags[27], or capture and concentration of labelled streptavidin[28].

The experiments shown here are the results of an initial round of parameter optimization. To achieve efficient pick-up of nanospheres, the speed of microtubules was adjusted to 100–150 nm s^{-1} by controlling the caged ATP concentration and light dosage. The biotinylation ratio of microtubules was reduced to 6%, because higher ratios of biotin–tubulin to unmodified tubulin resulted in impaired motility. The signal from GST capture was improved when the GST analyte was present in large excess of the antibody-labelled quantum dots (35-fold excess is better than threefold excess). The concentration of solutions, the incubation times and the number of wash steps between assembly steps were optimized. The microfabrication process was optimized to prevent delamination of the thick SU8 resist and to create the overhang at the wall.

The kinesin-powered smart dust biosensor is a significant step towards mimicking the autonomous, micrometre-sized, multifunctional sensors engineered by nature. In order to apply such smart dust biosensors in a practical setting, the design requires further iterations to improve specific processes as well as their integration. For example, opaque material covering the tagging zone will ensure that only fluorescent tags transported to the peripheral detection zone and a negligible fraction of the freely diffusing tags contribute to the sensor signal. In addition, strategies to manufacture, package and store[21,22] such devices at high yield and low cost need to be developed and taken into consideration in the design process. The performance has to be optimized and matched to specific application scenarios. Multiplexing can be achieved by

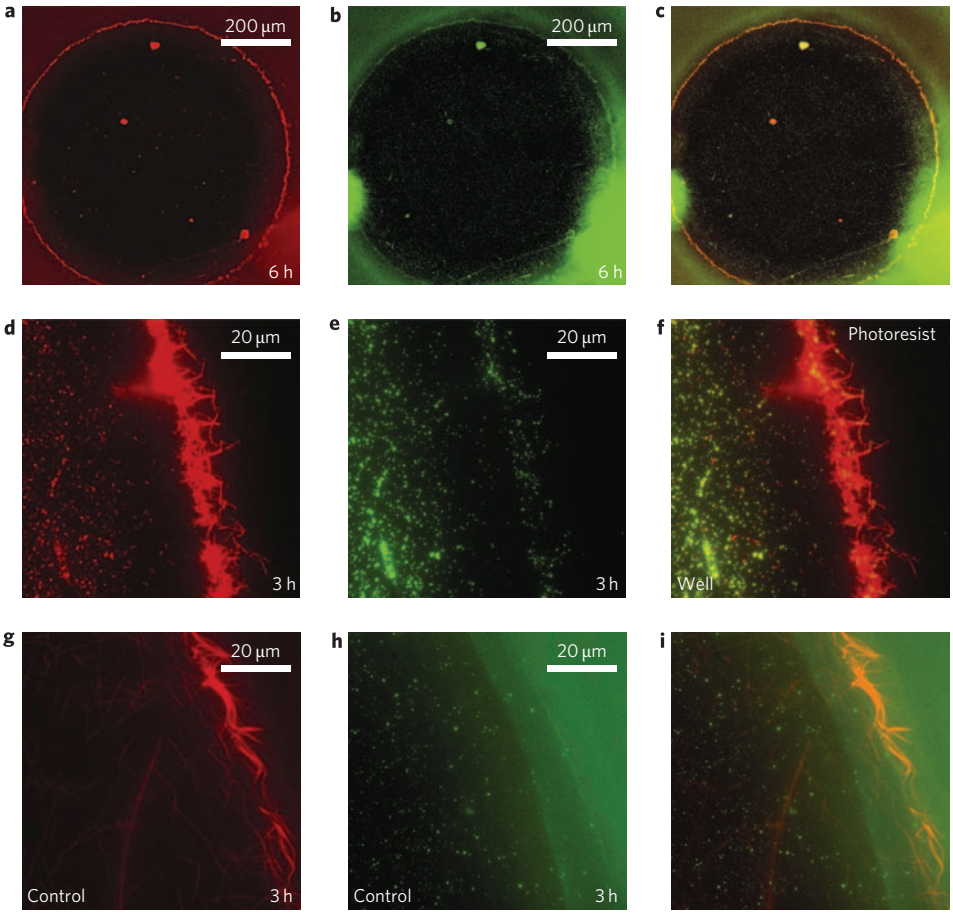

Figure 2 | Experimental results for streptavidin as analyte. a–i, Six hours after analyte introduction, microtubules (**a**) have aggregated at the wall, depositing along with them a ring of nanospheres (**b**) indicating the presence of streptavidin. Imaging the peripheral region at higher magnification 3 h after the start of the experiment reveals microtubule (**d**) and nanosphere (**e**) aggregation at the wall. The distinct transition between the capture/tag region and the deposition region is also apparent in **e**. In the absence of streptavidin, microtubules accumulate (**g**) but do not deposit nanospheres (**h**). Relative localization of microtubules and nanospheres is shown in **c**, **f** and **i**.

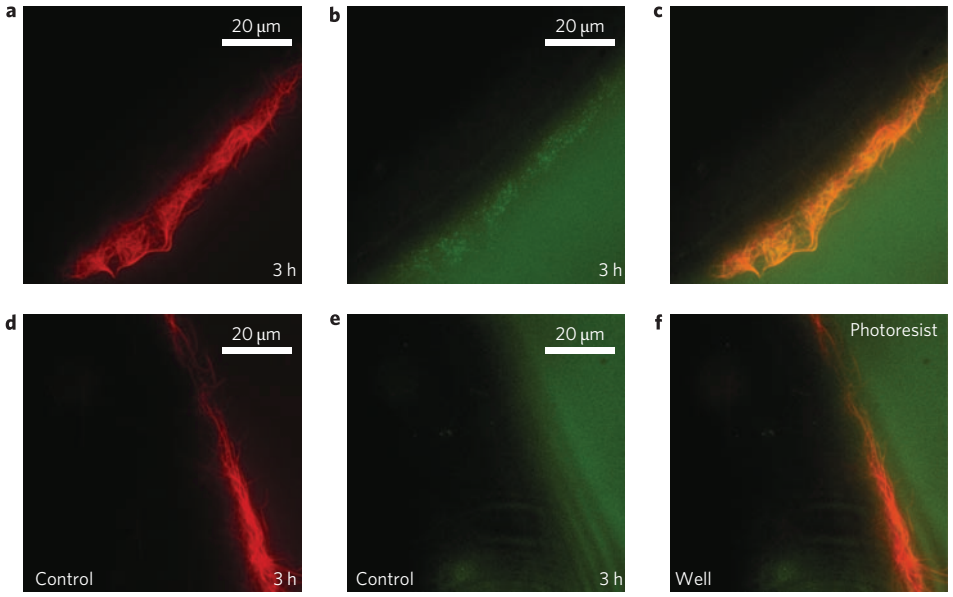

Figure 3 | Experimental results for GST as analyte. a–f, Microtubules functionalized with anti-GST antibodies and rhodamine have aggregated at the wall 3 h into the experiment (**a**) after capturing GST and anti-GST antibody conjugated quantum dots from the solution and depositing them at the wall (**b**). In the absence of GST, microtubules accumulate (**d**) but do not deposit quantum dots (**e**). Relative localization of microtubules and quantum dots is shown in **c** and **f**.

preparing devices with different antibody pairs and spectrally separable optical tags[29] and mixing the devices in the desired combinations. In summary, although centimetre-sized radio-frequency identification devices are beginning to penetrate the market, the design of submillimetre-sized distributed sensors for biomedical and biodefense applications is a new frontier in engineering to which biomimetic and hybrid systems offer interesting solutions.

Methods

A detailed description of the experimental procedure can be found in the Supplementary Information.

Photolithography. Round No. 2 cover slips serving as substrate were cleaned and baked. Approximately 1 ml of SU8-2015 photoresist was spin-coated onto the substrate, soft-baked, exposed through a printed photomask, post-baked, developed, rinsed and dried. The immobilization of microtubules at the sidewall is likely a result of nanoscale, wedge-shape gaps between the glass surface and the photoresist[25].

Kinesin preparation. A kinesin construct consisting of the wild-type, full-length *Drosophila melanogaster* kinesin heavy chain and a C-terminal His-tag was expressed in *Escherichia coli* and purified using a Ni-NTA column[30].

General assembly of the smart dust sensor. The assembly and operation of the smart dust sensor was carried out under minimal illumination to prevent accidental release of caged ATP. To prevent drying, degradation and photobleaching, the sensor was also kept under an atmosphere of humidified nitrogen except for the solution exchange steps. Solution exchange on the sensor surface was carried out manually using two 100-μl piston-driven air displacement pipettes. All solutions were applied as droplets onto the sensor surface and exchanged by suctioning the existing droplet and deposition of a new droplet.

Assembly of the streptavidin-specific smart dust sensor. Rhodamine-labelled microtubules and biotin-labelled microtubules were prepared by polymerizing rhodamine-labelled and biotinylated tubulin, respectively, and subsequently diluted 100-fold into BRB80 buffer (80 mM PIPES, 1 mM EGTA, 1 mM $MgCl_2$, pH 6.9) containing 10 μM paclitaxel.

The surfaces of the sensor were wetted for 5 min with BRB80 (100 μl), coated for 5 min with casein (0.5 mg ml^{-1} in BRB80, 100 μl) and for 10 min with kinesin (~10 nM in BRB80 with 0.5 mg ml^{-1} casein and 0.1 mM DMNPE-caged ATP, 100 μl). The surface was then washed once with antifade solution (0.2 mg ml^{-1} casein, 0.1 mM DMNPE-caged ATP, 20 mM D-glucose, 20 μg ml^{-1} glucose oxidase, 8 μg ml^{-1} catalase and 10 mM dithiothreitol (DTT) in BRB80, 100 μl). The surface was incubated for 5 min with a motility solution containing biotinylated and rhodamine-labelled microtubules (ratio 10:1, 16.0 μg ml^{-1} biotinylated microtubules, 1.6 μg ml^{-1} rhodamine-labelled microtubules, 0.1 mg ml^{-1} casein, 0.1 mM DMNPE-caged ATP, antifade system in BRB80, 100 μl). The surface was washed again with antifade solution (100 μl) and incubated for 5 min with a suspension (100 μl) containing 0.5 nM biotinylated fluorescent microspheres (diameter 40 nm, FluoSpheres F8766, Molecular Probes). After washing the surface twice with antifade solution (2× 100 μl) and incubating it with antifade solution (100 μl) the sensor was ready for operation.

Operation of the streptavidin-specific smart dust sensor. An analyte solution of Alexa Fluor 568-labelled streptavidin (Invitrogen) was loaded by solution exchange (1.0 nM streptavidin in antifade solution, 100 μl). For the control experiment, this step was omitted. Caged ATP was subsequently released by illuminating the sensor for 90 s with UV light (1.4 mW cm^{-2} intensity).

Assembly of the glutathione-S-transferase-specific smart dust sensor. Mixed microtubules (13% rhodamine, 6% biotin) were prepared by polymerizing a mixture of unlabelled, rhodamine-labelled and biotinylated tubulin and subsequently diluting 100-fold into BRB80 containing 10 μM paclitaxel. Rhodamine microtubules were prepared as described above.

The surfaces of the sensor were wetted, coated with casein and kinesin, and washed three times (as described above). The surface was then incubated for 10 min with a motility solution containing mixed and rhodamine-labelled microtubules (ratio 50:1, 15.0 μg ml^{-1} biotinylated microtubules, 0.3 μg ml^{-1} rhodamine-labelled microtubules, 0.1 mg ml^{-1} casein, 50 μM ATP, 20 mM D-glucose, 20 μg ml^{-1} glucose oxidase, 8 μg ml^{-1} catalase and 10 mM DTT in BRB80, 100 μl). The surface was again washed three times and incubated for 10 min with a solution of 8 nM unlabelled streptavidin in antifade solution (100 μl). Thereafter the surface was washed three times and incubated for 10 min with a solution of 32 nM biotinylated anti-GST in antifade solution (100 μl). Finally, the surface was washed three times and incubated with a suspension of 0.2 nM anti-GST-conjugated Qdot 655 in antifade solution (50 μl) for a final quantum dot concentration of 0.1 nM.

Operation of the glutathione-S-transferase-specific smart dust sensor. GST analyte was loaded at a final concentration of 4 nM by introducing 50 μl of 7.7 nM GST in antifade solution without mixing. For the control experiment, this step was omitted. Caged ATP was released after 25 min by illuminating the sensor for 240 s with UV light (1.4 mW cm^{-2} intensity).

Read out of the smart dust sensor. Read out was performed with a fluorescence microscope equipped with a ×100 oil objective (NA 1.4), a ×10 air objective (NA 0.3), and an electron multiplying charge coupled device (EMCCD) camera. To image microtubules and Alexa Fluor 568-labelled streptavidin a rhodamine cube (Excitation 535 nm, Emission 610 nm), for FluoSpheres a fluorescein filter cube (Excitation 480 nm, Emission 535 nm), and for Qdots 655 a modified Qdot cube (Excitation 420 nm, Emission 655 nm) were used.

Received 18 July 2008; accepted 1 December 2008; published online 18 January 2009

References

1. Kahn, J. M., Katz, R. H. & Pister, K. S. J. Emerging challenges: Mobile networking for 'smart dust'. *J. Commun. Netw.* **2,** 188–196 (2000).
2. Link, J. R. & Sailor, M. J. Smart dust: Self-assembling, self-orienting photonic crystals of porous Si. *Proc. Natl Acad. Sci. USA* **100,** 10607–10610 (2003).
3. Sailor, M. J. & Link, J. R. 'Smart dust': nanostructured devices in a grain of sand. *Chem. Commun.* 1375–1383 (2005).
4. Soong, R. K. *et al.* Powering an inorganic nanodevice with a biomolecular motor. *Science* **290,** 1555–1558 (2000).
5. Hiratsuka, Y., Tada, T., Oiwa, K., Kanayama, T. & Uyeda, T. Q. Controlling the direction of kinesin-driven microtubule movements along microlithographic tracks. *Biophys. J.* **81,** 1555–1561 (2001).
6. Hess, H., Clemmens, J., Qin, D., Howard, J. & Vogel, V. Light-controlled molecular shuttles made from motor proteins carrying cargo on engineered surfaces. *Nano Lett.* **1,** 235–239 (2001).
7. Nicolau, D. V., Suzuki, H., Mashiko, S., Taguchi, T. & Yoshikawa, S. Actin motion on microlithographically functionalized myosin surfaces and tracks. *Biophys. J.* **77,** 1126–1134 (1999).
8. Bunk, R. *et al.* Towards a 'nano-traffic' system powered by molecular motors. *Microelectron. Eng.* **67–68,** 899–904 (2003).
9. Hess, H., Bachand, G. D. & Vogel, V. Powering nanodevices with biomolecular motors. *Chem. Eur. J.* **10,** 2110–2116 (2004).
10. van den Heuvel, M. G. L. & Dekker, C. Motor proteins at work for nanotechnology. *Science* **317,** 333–336 (2007).
11. Dennis, J. R., Howard, J. & Vogel, V. Molecular shuttles: directed motion of microtubules along nanoscale kinesin tracks. *Nanotechnology* **10,** 232–236 (1999).
12. Bachand, G. D., Rivera, S. B., Carroll-Portillo, A., Hess, H. & Bachand, M. Active capture and transport of virus particles using a biomolecular motor-driven, nanoscale antibody sandwich assay. *Small* **2,** 381–385 (2006).
13. Ramachandran, S., Ernst, K.-H., Bachand, G. D., Vogel, V. & Hess, H. Selective loading of kinesin-powered molecular shuttles with protein cargo and its application to biosensing. *Small* **2,** 330–334 (2006).
14. Diez, S. *et al.* Stretching and transporting DNA molecules using motor proteins. *Nano Lett.* **3,** 1251–1254 (2003).
15. Taira, S. *et al.* Selective detection and transport of fully matched DNA by DNA-loaded microtubule and kinesin motor protein. *Biotechnol. Bioeng.* **95,** 533–538 (2006).
16. Hirabayashi, M. *et al.* Malachite green-conjugated microtubules as mobile bioprobes selective for malachite green aptamers with capturing/releasing ability. *Biotechnol. Bioeng.* **94,** 473–480 (2006).
17. Taira, S. *et al.* Loading and unloading of molecular cargo by DNA-conjugated microtubule. *Biotechnol. Bioeng.* **99,** 734–739 (2008).
18. Lin, C.-T., Kao, M.-T., Kurabayashi, K. & Meyhofer, E. Self-contained, biomolecular motor-driven protein sorting and concentrating in an ultrasensitive microfluidic chip. *Nano Lett.* **8,** 1041–1046 (2008).
19. Wu, D., Tucker, R. & Hess, H. Caged ATP: Fuel for bionanodevices. *IEEE Trans. Adv. Packag.* **28,** 594–599 (2005).
20. Tucker, R., Katira, P. & Hess, H. Herding nanotransporters: Localized activation via release and sequestration of control molecules. *Nano Lett.* **8,** 221–226 (2008).
21. Seetharam, R., Wada, Y., Ramachandran, S., Hess, H. & Satir, P. Long-term storage of bionanodevices by freezing and lyophilization. *Lab. Chip* **6,** 1239–1242 (2006).
22. Uppalapati, M., Huang, Y. M., Jackson, T. N. & Hancock, W. O. Enhancing the stability of kinesin motors for microscale transport applications. *Lab. Chip* **8,** 358–361 (2008).
23. Sheehan, P. E. & Whitman, L. J. Detection limits for nanoscale biosensors. *Nano Lett.* **5,** 803–807 (2005).
24. Nitta, T., Tanahashi, A., Hirano, M. & Hess, H. Simulating molecular shuttle movements: Towards computer-aided design of nanoscale transport systems. *Lab. Chip* **6,** 881–885 (2006).
25. Stracke, P., Bohm, K. J., Burgold, J., Schacht, H. J. & Unger, E. Physical and technical parameters determining the functioning of a kinesin-based cell-free motor system. *Nanotechnology* **11,** 52–56 (2000).

26. Finger, I., Phillips, S., Mobley, E., Tucker, R. & Hess, H. Absolute brightness of fluorescent microspheres. *Lab. Chip* doi: 10.1039/B810219H (2009).
27. Brunner, C., Wahnes, C. & Vogel, V. Cargo pick-up from engineered loading stations by kinesin driven molecular shuttles. *Lab. Chip* **7,** 1263–1271 (2007).
28. Lin, C. T., Kao, M. T., Kurabayashi, K. & Meyhofer, E. Self-contained biomolecular motor-driven protein sorting and concentrating in an ultrasensitive microfluidic chip. *Nano Lett.* **8,** 1041–1046 (2008).
29. Han, M. Y., Gao, X. H., Su, J. Z. & Nie, S. Quantum-dot-tagged microbeads for multiplexed optical coding of biomolecules. *Nature Biotechnol.* **19,** 631–635 (2001).
30. Coy, D. L., Hancock, W. O., Wagenbach, M. & Howard, J. Kinesin's tail domain is an inhibitory regulator of the motor domain. *Nature Cell Biol.* **1,** 288–292 (1999).

Acknowledgements

This work is part of a collaborative project with G. D. Bachand, V. Vogel, B. Ratna and P. Satir, whose insights and contributions are gratefully acknowledged. Financial support was provided by the Defense Advanced Research Project Agency (DARPA) Biomolecular Motors Program (Air Force Office of Scientific Research (AFOSR) FA9550-05-1-0274 and FA9550-05-1-0366) and the University of Florida (UF) Centre for Sensor Materials and Technologies (ONR N00014-07-1-0982). T.F. was partially supported by a Feodor Lynen fellowship from the Alexander von Humboldt foundation. The authors would also like to thank A. Ogden from the UF Nanofabrication Centre for his advice and support.

Author contributions

T.F., A.A. and H.H. conceived and designed the experiments. T.F. and A.A. performed the experiments and analysed the data. All authors discussed the results. T.F., A.A. and H.H. co-wrote the paper.

Additional information

Supplementary Information accompanies this paper at www.nature.com/naturenanotechnology. Reprints and permission information is available online at http://npg.nature.com/reprintsandpermissions/. Correspondence and requests for materials should be addressed to H.H.